



NORSAR Scientific Report No. 1-1999/2000

Semiannual Technical Summary

1 April - 30 September 1999

Kjeller, November 1999

6.1 Earthquake location accuracies in Norway based on a comparison between local and regional networks

Abstract

Detailed studies of the low to intermediate seismicity in two coastal regions of Norway have been used in a comparison between earthquake locations from local high-precision networks on the one side and locations using a sparse regional array network on the other side. To this end, a reference set of 32 low-magnitude earthquakes have been located using two local temporary networks in northern and western Norway, with estimated epicenter accuracies better than 5 and 10 km, respectively. Comparisons are made between the local network solutions and the NORSAR Generalized Beamforming (GBF) system, which provides automatic phase association and location estimates using the Fennoscandian regional array network. The median automatic GBF location error is of the order of 20-30 km when four or more arrays detect the event, increasing to about 80-100 km when only two arrays are available, and the automatic GBF bulletin is essentially complete down to magnitude $M_L=2.0$. Most of the mislocation vectors of the NORSAR GBF solutions are oriented perpendicular to the Norwegian coast, and with a tendency to pull the location in a southeasterly direction. The GBF performance is clearly better, both in terms of accuracy and completeness, than the performance of the automatic bulletin of the Prototype International Data Center (PIDC) which uses data from essentially the same network. The analyst reviewed NORSAR and PIDC bulletins show, not unexpectedly, an improvement in location accuracy compared to the automatic solutions and appear to be of similar quality for the few common events, with an average mislocation of about 20 km. The NORSAR reviewed bulletin is more complete at low magnitudes compared to PIDC, and there appears to be a potential for significant improvements in the PIDC processing of small seismic events in this region.

Introduction

A considerable effort is currently taking place to develop and apply location calibration information for seismic events recorded by the International Monitoring System (IMS) for the Comprehensive Nuclear-Test-Ban Treaty (CTBT) (e.g., Bondar and North, 1999). One important source of such calibration information is sets of explosions or earthquakes with very accurate locations (so-called Ground Truth information). Earthquakes monitored by local microseismic networks with high location precision are in many cases appropriate as calibration events, and in this paper we present a number of earthquake hypocenters calculated from local networks in northern and western Norway (located within the two boxes in Fig. 1, where also the regional seismicity is shown). We use these results to evaluate the accuracy of automatic and interactive location estimates using a sparse regional array network, essentially comprising the IMS seismic stations in Fennoscandia. While most of our emphasis is on evaluating the NORSAR automatic processing system, we also compare the results with those of the automatic PIDC process, as well as with analyst reviewed results at NORSAR and the PIDC.

NORSAR and PIDC detection and location processing

The NORSAR automatic system makes use of the Generalized Beamforming (GBF) method, which was developed by Ringdal and Kværna (1989), and which has been applied routinely at

NORSAR since 1990. The GBF algorithm is based upon processing data from a sparse network of regional arrays, and associates detected phases by forming a regional grid system and "steering" the network towards each individual grid point. Each detected phase at one of the arrays is treated as a 0-1 valued function, where the value 1 is assigned if the detection corresponds in azimuth and slowness to the grid point. By simply adding these functions, suitably delayed in time, one obtains an efficient phase association of seismic events as well as a preliminary location. By using a denser grid ("beampacking") around this initial epicenter, the location estimates are subsequently refined.

The automatic association and event definition procedure at the PIDC makes use of the same basic principles as the NORSAR GBF, but introduces a set of weighting criteria (different from the 0/1 weightings used at NORSAR) in the beamforming procedure. A seismic event is defined when the weighted sum of detected phases exceeds a predefined threshold. The threshold setting represents a tradeoff between the desire for completeness (no missed events) and for avoiding spurious events (false associations). In contrast to the NORSAR GBF, the threshold at the PIDC is set to a relatively high value in order to minimize the number of spurious (false) events. On the other hand, this results in several real seismic events being missed by the PIDC automatic procedure, as will be further shown by examples in this paper.

The Local Networks and their Capabilities

The two local networks studied in this paper are located in the Ranafjord area (northern Norway) and the Bremanger area (western Norway). Fig. 1 shows the two study areas along with a seismicity map of Fennoscandia. The technical installations for both networks are similar, relying on radio links to transmit data to a central station, where the data are digitized, and a real-time STA/LTA analysis is performed by a local, PC-based acquisition system (Hicks et al., 1999a). Triggers are stored locally and downloaded to NORSAR on a daily basis. Sampling rates are 40 Hz for both networks. Whenever convenient, the readings from the two networks have been supplemented by readings from nearby permanent seismic stations part of the National Norwegian Seismic Network. However, these additional stations did not provide any significant improvement of the locations, but rather acted as confirmation.

The Ranafjord network (Fig. 2) comprised initially six seismic stations installed in June 1997 as part of a research project (NEONOR, Neotectonics in Norway), with the main purpose of monitoring possibly seismic activity along potentially active local faults (Hicks et al., 1999a). The network was reduced to four stations in September 1998, but without significant loss in location precision. The Bremanger network (Fig. 3) has been in operation since October 1998, but has not been operating continuously since it was installed, and less data are therefore available here than one otherwise should have expected in view of the proximity to seismically active areas of the North Sea (Bungum et al., 1991).

The location algorithms used for both networks is a version of the Hypocenter program (Lienert et al., 1986), which uses scaled, adaptively damped least squares to determine hypocenter location. Due to the close distances from hypocenter to station, (5-40 km for the Rana network) the phase arrivals for events of this magnitude can be picked with a high accuracy. This is especially the case for the 'larger' events ($M_L > 1.5$) such as those used in this study. The short distances also mean that first arrivals are direct waves, so the only velocities used in the location are the upper 15 km of the crust. Consequently, RMS traveltimes residuals are less than 0.1s for all earthquakes in the Rana network, and generally less than 0.5s for the earthquakes in West-

ern Norway, using arrival times from the local and permanent networks. The velocity models used are fairly accurate for the relatively consistent geophysical properties in the areas surrounding the networks.

Based on a detailed analysis of the location error ellipsoids, we estimate that the accuracy of the epicenter locations in Rana is better than 5 km, and most likely within 2-3 km for the events near the network. The events located in the Bremanger area are somewhat farther from the network itself, and of higher magnitude. In this case there is, however, a more significant contribution from the permanent network, which is better in western than in northern Norway. A conservative estimate of the location accuracy near Bremanger would be between 5 and 10 km. This means that the local earthquakes from Rana and Bremanger will qualify as GT5 and GT10 events (GT = Ground Truth), i.e., with location accuracies better than 5 and 10 km, respectively.

Seismicity in and around the Local Networks

The offshore and onshore parts of Northern Norway have long been considered an area of elevated seismic activity with regard to the rest of the Baltic shield and margin areas, albeit not particularly high as compared to some other passive (rifted) continental margins globally (Bungum et al., 1991; Byrkjeland et al., in press). The largest known onshore earthquake in Fennoscandia in historical times occurred in the Ranafjord area, where the Rana network is located, on August 31, 1819, and with an estimated magnitude of M_S 5.8-6.2 (Muir Wood, 1989). This earthquake was felt over most of Fennoscandia, as far away as Stockholm and Oslo.

The northern parts of the North Sea, adjacent to the Bremanger network, are among the most seismically active areas in northern Europe, in a structurally very complex region. The largest recent earthquakes in this area occurred on August 8, 1988, and on January 23, 1989, with respective magnitudes of M_L 5.1 and 4.9 (Hansen et al., 1989). The 1988 earthquake occurred around 200 km northwest of the current network, while the 1989 earthquake was around 50 km due west of the current network.

Of the 420 events located by the Rana network, 340 are located in the immediate vicinity of the network, and 40 of these are confirmed explosions or probable explosions, leaving around 300 as probable earthquakes. Magnitudes range from M_L 0.1 to 2.8, with most events in the M_L 1.0 to 1.5 range. The hypocenter depths are shallow, mainly from 4 to 12 km, thereby indicating that this is essentially a swarm activity of the type seen also elsewhere in this region (Bungum et al., 1979; Atakan et al., 1994).

Fig. 2 shows the 1997-1999 micro-seismic activity in the Rana region plotted according to magnitude (explosions removed). Five main groups of events are visible in the western part of the network. These groups occur as swarms, having well defined activity periods and hypocenter depths. The largest events within the network occurred within the two westernmost groups, which are also located in the vicinity of many of the reported phenomena concerning the 1819 earthquake. The easternmost group has hypocenter depths predominantly around 4-6 km, while the other three mainland groups mainly have depths in the 10-12 km range. The depth estimate for the large westernmost group is slightly more uncertain since these events lie further outside the network, but since several of the earthquakes were noticed as loud bangs/cracking noises the depths are most likely less than five km for this group also.

Focal mechanism solutions determined using data from the Rana network show an σ_{Hmax} orientation parallel to the coast, which is a 90° rotation with respect to the regional, ridge push dominated, stress field (Hicks et al., 1999b). This implicates a strong local stress influence on the seismic activity in the area. The northern North Sea is a geologically very complex area, with an intricate system of rifted basins and highs. However, focal mechanisms in this area do largely comply with the expected direction of the ridge push force, although some mechanisms southwest of the network (Lindhölm et al.; in press) do have a similar inversion of the σ_{Hmax} direction as seen in the Rana area.

The Bremanger area has of yet not shown any clear patterns of seismicity, the activity appears to be fairly well distributed, as shown in Fig. 3. The largest earthquake (M_L 3.9) located occurred in an area where there has been no earlier known activity. The other two earthquakes with magnitudes larger than 2.0 occurred within the areas known to have the highest seismic activity from earlier instrumental data.

Location Results using the Regional Array Network

A total of 32 of the local earthquakes detected by the local networks were also detected and located by NORSAR's automatic GBF system. Of these, 21 were reviewed by the NORSAR analysts. Eight events were detected by the PIDC automatic bulletin, six of which were reviewed. All of these events are listed in Table 1, together with locations and location differences. For the Rana region the details of the magnitude information are given in Fig. 4, where it is seen that the PIDC system has a detection threshold near M_L 2.5 (but with two missing M_L 2.7 events), while the GBF system seems to have a detection threshold of about M_L 2.0 (but with one missing M_L 2.1 event).

The location differences are plotted vs. number of stations used in the solution in Fig. 5, with a second order regression line for the GBF solutions, and the median location differences are also shown in the same figure. It can be inferred from these results that both the GBF and PIDC location accuracies are quite sensitive to number of stations used (and thereby event magnitude). In contrast, the NORSAR analyst reviewed solutions retain good accuracy (median error about 20 km) even for the smaller events, although events detected on only 1 or 2 stations are usually not reviewed. It is, however, because of the large scatter, difficult to use Fig. 5 in comparing the performance of the two systems in more detail, except that the analyst review causes a clear improvement in the location accuracies for both systems. Table 2 shows average location 'errors' for the five events for which all four types of solutions are available (all from Rana, see Table 1), and it appears that the GBF has better automatic solutions than the PIDC (32 versus 60 km) while the reviewed solutions are quite similar (22 versus 20 km). However, the low number of events in the PIDC bulletins combined with the large scatter makes it difficult to conclude very clearly here.

It can be seen from Table 1 (see also Fig. 5) that the automatic GBF system provides epicenters with median location error about 20-30 km for events that are detectable on four or more stations. For the smaller events, detectable at only 1 or 2 stations, the GBF location accuracy deteriorates, with a median error of about 80-100 km and with a large scatter. The azimuthal distribution of the location differences for the GBF solutions are shown in Fig. 6. The mislocation vectors are generally oriented NW-SE (perpendicular to the coast), and it is also apparent that the GBF system tends to bias the solutions towards the southeast, in particular for events with the largest uncertainties (fewer detecting stations).

Concluding Remarks

The following main conclusions can be drawn from this study of detection and location of small events in northern and western Norway:

- Using essentially the same network of seismic stations (arrays), the automatic NORSAR GBF is significantly better than the automatic PIDC system both in terms of location accuracy (~30 and ~60 km for common events) and detectability (M_L 2.0 and 2.5).
- The quality of the automatic GBF locations deteriorates quite rapidly when fewer stations are used in the solution, whereas the accuracy of the NORSAR analyst reviewed solutions remains high.
- The analyst reviewed NORSAR and PIDC bulletins have similar location accuracies (~20 km) for the few common events, but the NORSAR bulletin is more complete at low magnitudes.

In this paper we have sometimes used the term 'location error' or 'location accuracy' when comparing results from the local and regional networks. We note that the local network solutions, which have been used as reference, may themselves be mislocated by up to 5 or 10 km. The real performance of the regional network locations should therefore be slightly better than evaluated here. We should also note that the grid spacing for the GBF system is 33.3 km (0.3°), so the solutions within 20 km are therefore in general located to the closest grid point. Potentials for further improvements here are apparent. With respect to the PIDC solutions we finally note that, for the region considered in this paper, the only significant difference between the arrays and stations used by the two systems is that the PIDC system uses the large-aperture NOA array instead of the regional small-aperture NORES array. While this could explain some of the difference between the two systems, it seems that there should still be potentials for the PIDC to detect events at a lower magnitude level than what is done today, and possibly also with better precisions in its automatic solutions which are quite important in an operational situation within a CTBT context.

In closing we note that events located by local networks as analyzed here provide an interesting potential for extending the data base of Ground Truth events.

Acknowledgments

The NEONOR project, providing the local microearthquake networks used in this paper, has been supported by the Research Council of Norway, Amoco, Norsk Hydro, Phillips Petroleum, Statkraft, the Norwegian Petroleum Directorate, the Norwegian Geological Survey and NORSAR.

E.C. Hicks, NORSAR & Dept. for Geology, Univ. of Oslo
H. Bungum, NORSAR & Dept. for Geology, Univ. of Oslo
F. Ringdal

References

Atakan, K., C.D. Lindholm, and J. Havskov (1994): *Earthquake swarm in Steigen, Northern Norway: an unusual example of intraplate seismicity*, Terra Nova, 6, 180-194.

- Blystad, P., H. Brekke, R.B. Færseth, B.T. Larsen, J. Skogseid, and B. Tørudbakken (1995): *Structural elements of the Norwegian continental shelf, Part II: The Norwegian Sea region*, NPD Bulletin, 8.
- Bondar, I. and R.G. North (1999): *Development of calibration techniques for the Comprehensive Nuclear-Test-Ban Treaty (CTBT) international monitoring system*. Phys. Earth. Plan. Int., 113, 11-24.
- Bungum, H., A. Alsaker, L.B. Kvamme, and R.A. Hansen (1991): *Seismicity and seismotectonics of Norway and surrounding continental shelf areas*, J. Geophys. Res., 96, 2249-2265.
- Bungum, H., B.K. Hokland, E.S. Husebye, and F. Ringdal (1979): *An exceptional intraplate earthquake sequence in Meløy, Northern Norway*, Nature, 280, 32-35.
- Byrkjeland, U., H. Bungum, and O. Eldholm (in press): *Seismotectonics of the Norwegian margin*, J. Geophys. Res.
- Hansen, R.A., H. Bungum, and A. Alsaker (1989): *Three recent larger earthquakes offshore Norway*, Terra Nova, 1, 284-295.
- Hicks, E., H. Bungum, and C.D. Lindholm (1999a): *Seismic activity, inferred from crustal stresses and seismotectonics in the Rana region, Northern Norway*, Quaternary Sci. Rev., in press.
- Hicks, E., H. Bungum, and C.D. Lindholm (1999b): *Crustal stresses in Norway and surrounding areas as derived from earthquake focal mechanism solutions and in-situ stress measurements*, Nor. Geol. Tidsskr., submitted.
- Lienert, B.R.E., E. Berg, and L.N. Frazer (1986): *Hypocentre: An earthquake location method using centered, scaled and adaptively damped least squares*, Bull. Seis. Soc. Am., 76, 771-783.
- Lindholm, C.D., H. Bungum, E. Hicks, and M. Villagran (in press): *Crustal stress and tectonics in Norwegian regions determined from earthquake focal mechanisms*, Geol. Soc. Lond., Spec. Publ.
- Muir Wood, R. (1989): *The Scandinavian Earthquakes of 22 December 1759 and 31 August 1819*, Disasters, 12, 223-236.
- Ringdal, F. and T. Kværna (1989): *A multichannel processing approach to real time network detection, phase association and threshold monitoring*, Bull. Seism. Soc. Am., 79, 1927-1940.
- Vaage, S. (1980): *Seismic evidence of complex tectonics in the Meløy earthquake area*, Nor. Geol. Tidsskr., 60, 213-217.

Table 1

Date & time	Local solutions				NORSAR GBF			NORSAR reviewed			PIDC automatic (SEL1)			PIDC reviewed (REB)		
	Mag	Depth	Lat.	Lon.	Δ (km)	azi	nsta	Δ (km)	azi	nsta	Δ (km)	azi	nsta	Δ (km)	azi	nsta
99.05.29 - 00:31:44	3.9	8.7	62.189	4.741	22.6	234.2	7	20.5	65.2	8	52.3	355.8	3	24.5	210.0	8
98.06.18 - 22:54:00	2.7	11.4	66.376	13.111	22.1	97.3	5				39.3	111.3	1	59.0	78.5	3
98.12.16 - 20:57:46	2.7	8.7	66.270	12.983	36.8	131.6	5	30.5	102.4	5						
98.10.26 - 13:17:22	2.5	4.0	66.227	13.050	31.4	128.7	5	28.5	116.5	5	98.8	170.9	2	9.2	28.1	4
99.02.25 - 14:11:43	2.3	4.9	66.295	13.247	17.0	68.7	5	39.9	112.1	5	31.4	74.9	2			
98.02.09 - 12:59:05	2.8	10.7	66.385	13.088	56.6	93.4	4	22.3	114.7	6	55.5	94.4	2	24.6	100.2	4
98.03.09 - 14:19:57	2.8	6.6	65.854	13.529	37.1	107.8	4	5.6	93.4	6	54.7	68.3	3	2.1	190.5	4
97.11.25 - 22:24:17	2.7	11.0	66.500	12.403	88.5	100.0	4	15.4	118.4	5						
97.11.21 - 18:00:09	2.3	6.3	66.413	13.222	31.2	328.1	4	2.7	163.5	5						
98.10.13 - 22:21:59	2.3	3.0	66.241	13.015	14.2	328.7	4	34.7	101.3	4	36.8	98.6	2	38.2	112.0	4
99.01.07 - 14:04:13	2.3	0.0	66.856	13.894	21.4	60.5	4	45.5	108.0	4	11.9	83.4	2			
99.04.13 - 21:31:40	2.3	0.1	66.368	13.218	35.5	332.7	4	9.4	72.6	4						
98.10.29 - 21:07:29	2.3	3.0	66.222	13.045	21.1	204.8	4	36.2	102.6	4						
98.01.08 - 08:04:46	2.2	12.8	66.368	13.134	33.9	338.2	4	11.7	105.9	4						
98.01.11 - 20:01:18	2.2	12.3	66.373	13.110	33.0	339.6	4	16.0	105.6	4						
98.08.11 - 18:52:27	2.1	12.3	66.360	13.144	13.7	265.5	4									
98.12.24 - 07:50:10	2.1	16.6	66.395	13.288	14.8	109.6	4	18.6	79.1	4						
98.10.26 - 22:56:19	2.0	3.0	66.224	13.041	44.5	288.8	4	28.7	115.5	5						
99.06.26 - 21:30:46	2.5	23.7	61.728	4.274	23.4	47.2	3	10.2	167.3	2						
98.02.04 - 14:31:40	2.3	10.6	66.382	13.091	56.5	93.0	3	18.3	128.4	3						
98.12.04 - 12:39:29	2.3	22.2	66.163	12.275	103.0	115.6	3									
98.10.29 - 05:59:53	2.0	3.0	66.228	13.048	16.3	326.9	3	36.2	103.7	4						
98.12.05 - 22:14:53	1.9	13.0	66.751	13.812	26.3	115.1	3	23.4	102.2	4						
99.06.15 - 01:12:57	2.4	13.7	61.947	4.621	24.7	249.9	2	7.3	236.5	2						
98.02.28 - 16:53:26	2.0	11.6	66.701	13.316	179.3	90.0	2									
98.12.16 - 19:57:46	2.0	0.0	66.272	12.924	67.7	110.8	2									
99.04.09 - 08:04:28	2.0	8.0	66.389	13.351	159.0	115.2	2									
98.10.09 - 05:30:14	1.8	3.0	66.249	12.981	45.5	118.8	2									
98.12.17 - 18:33:24	1.8	0.0	66.262	13.000	181.7	118.3	2									
98.10.23 - 02:50:21	1.8	3.0	66.259	13.000	64.0	110.8	2									
98.12.21 - 17:09:47	1.6	33.0	66.488	14.259	161.3	119.3	2									
99.05.15 - 05:50:29	1.3	8.2	61.523	4.844	31.5	102.6	1									

Table 6.1.1. *Locations and location differences for the 32 events in this study. The reference locations are from the solutions determined by the local networks, where solutions north of 65°N are from Rana (six stations, four since September, 1998), the remaining from Bremanger (also six stations). Solutions using a sparse regional network (NORSAR, automatic (GBF) and reviewed; PIDC, automatic and reviewed) are given by location difference (Δ) in km, and azimuth, both compared to the local solution. The number of stations used in each case is also included. The events are sorted by number of stations in the GBF solution.*

Regional network location	Average location difference (km)
NORSAR GBF automatic	32 \pm 16
PIDC automatic	60 \pm 23
NORSAR reviewed	22 \pm 11
PIDC reviewed (REB)	20 \pm 14

Table 6.1.2. *Average location difference, with standard deviations, for five events from the Rana region covered by all solutions (see Table 6.1.1), between the local network solutions (location error less than 5 km) and the four regional network solutions, NORSAR and PIDC, automatic and reviewed.*

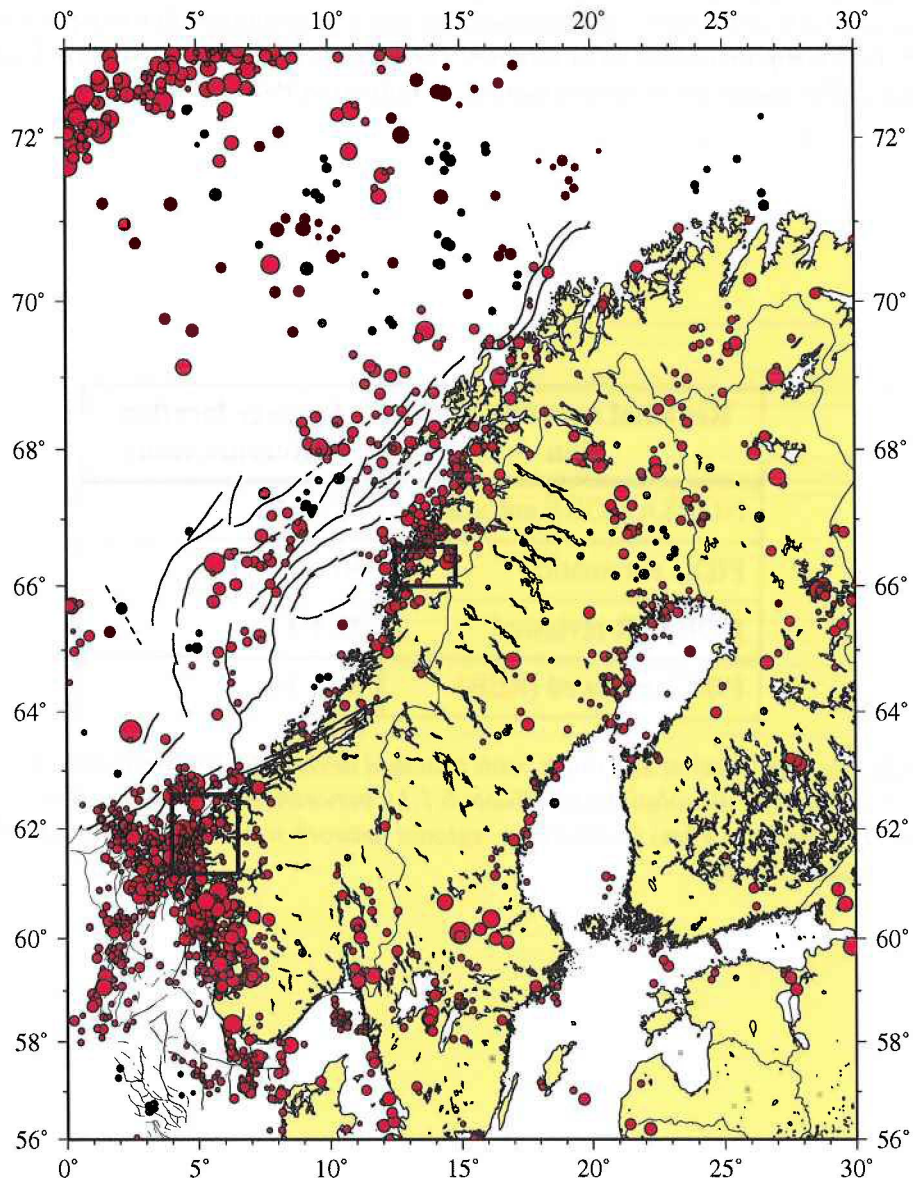


Fig. 6.1.1. Seismic activity in Norway 1980-1999, $M_w > 2.0$. The locations of the two study areas in this paper, Rana and Bremanger, are shown by the two rectangles in northern and western Norway, respectively. Structural information is from Blystad et al. (1995).

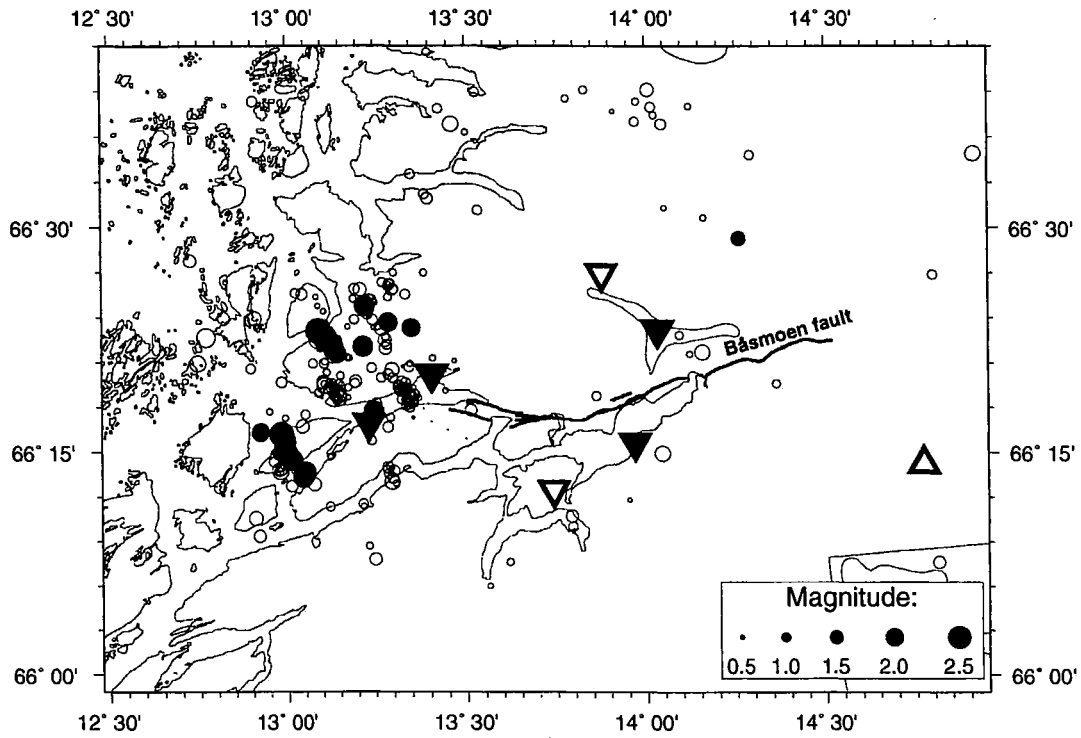


Fig. 6.1.2. Local seismic activity located by the Rana network 1997-1999. The filled circles represent the events also located by the NORSAR GBF system. The stations are indicated by inverted triangles, the four stations remaining after September 1998 are filled. The three-component MOR8 station that is part of the national Norwegian seismic network, operated by the University of Bergen, is shown by a triangle to the east in the figure. The solid black line is the postglacial Båsmoen fault, considered to be potentially seismically active.

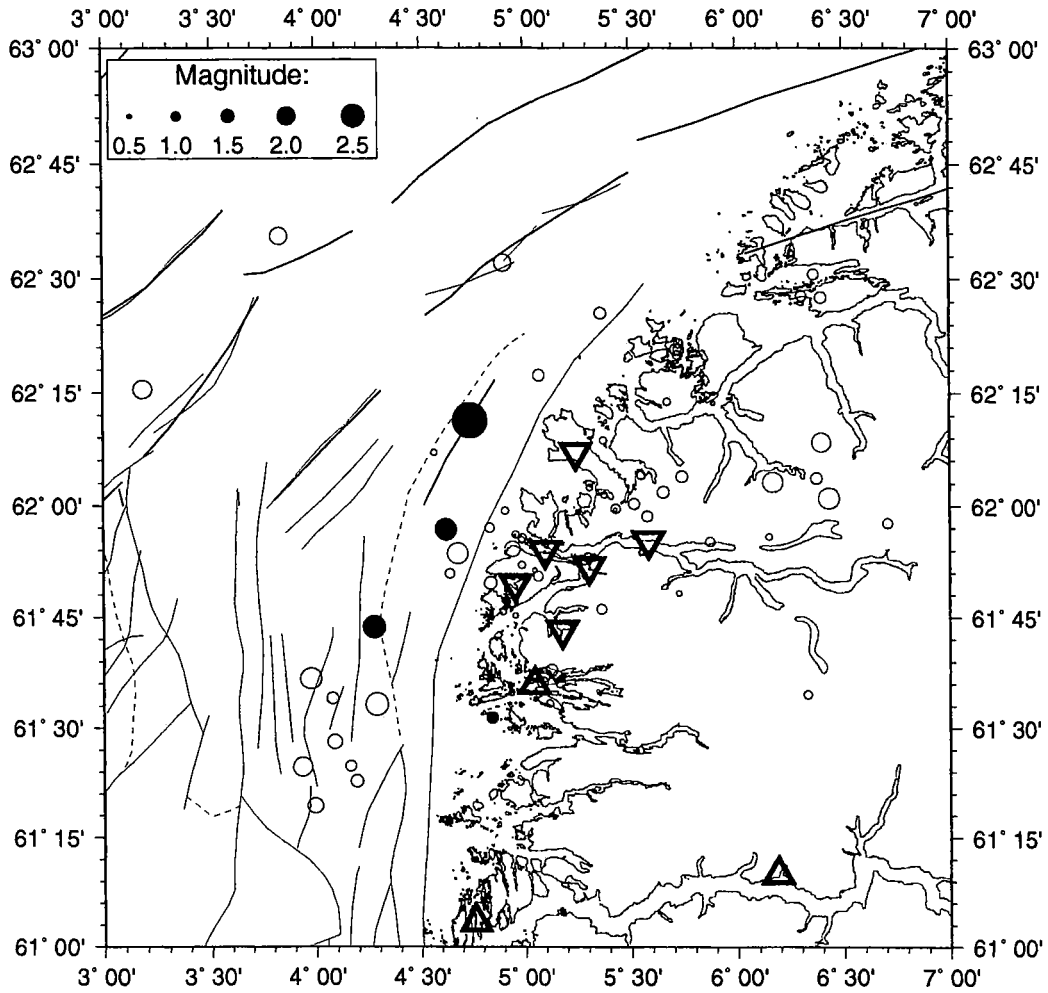


Fig. 6.1.3. Local seismic activity located by the Bremanger network, 1998-1999. The filled circles represent the earthquakes also located by the NORSAR GBF system. The stations in the local network are indicated by inverted triangles. The NNSN stations in the area are shown as triangles.

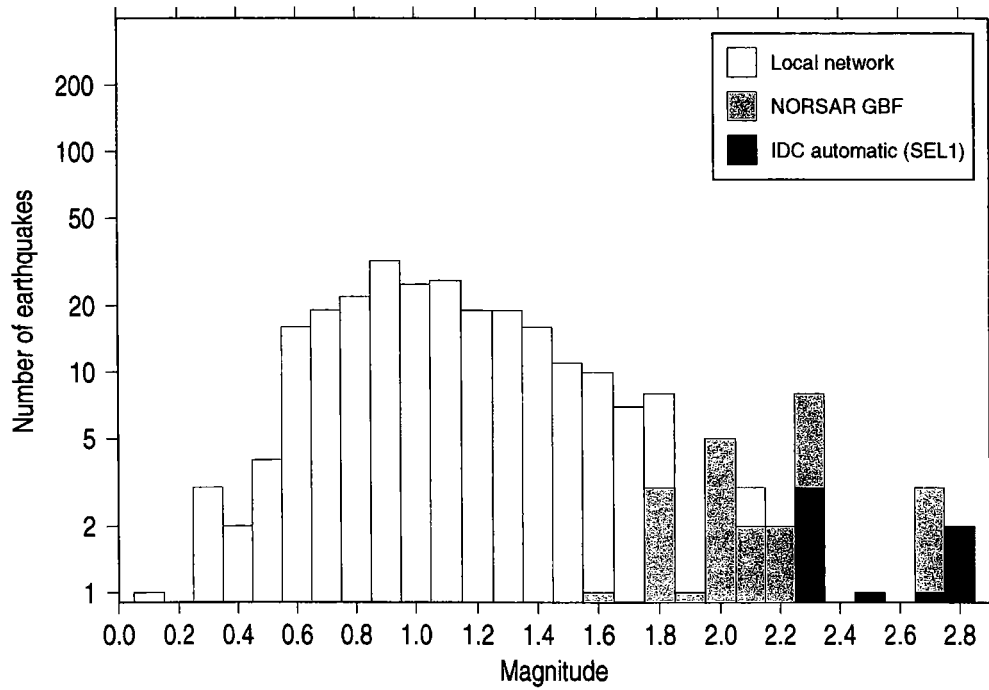


Fig. 6.1.4. Histogram of frequency-magnitude distribution for the Rana local seismic network (based on about two years of operation) together with events reported by the automatic NORSAR GBF (Generalized Beamforming) system (shaded) and the automatic PIDC (Prototype International Data Center) system (black).

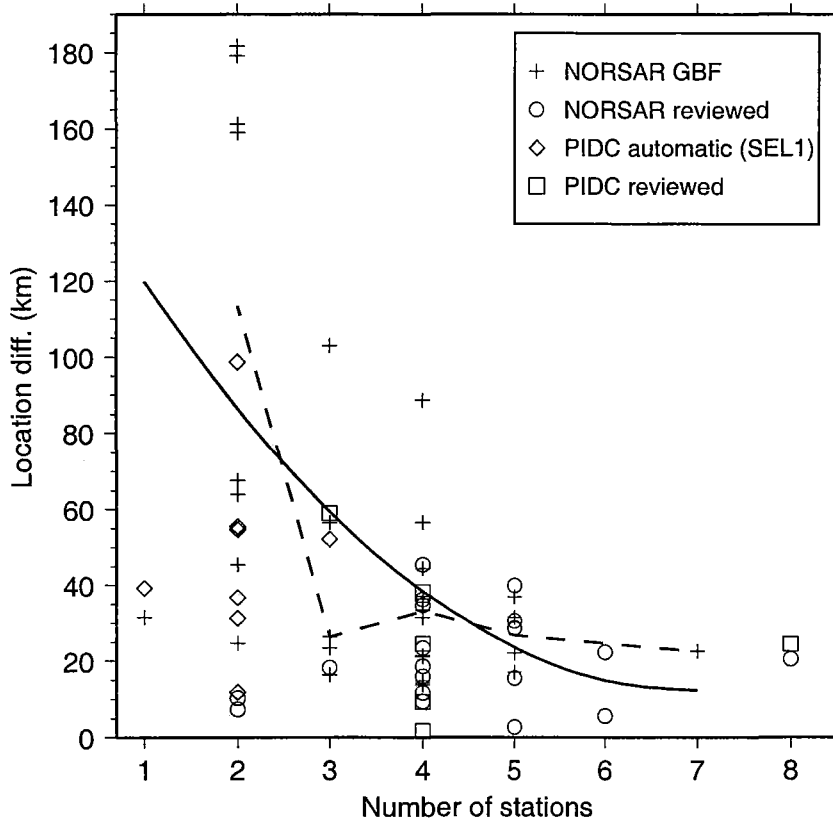


Fig. 6.1.5. Scatter plot of the location differences between the local network locations and the NORSAR GBF (automatic) solutions (circles), the PIDC automatic (diamonds) and the PIDC reviewed (squares) solutions, respectively, plotted vs. number of stations used in the solution. A second order regression analysis for the GBF solutions is shown by the solid line, while the dashed line represents the median differences for the GBF solutions.

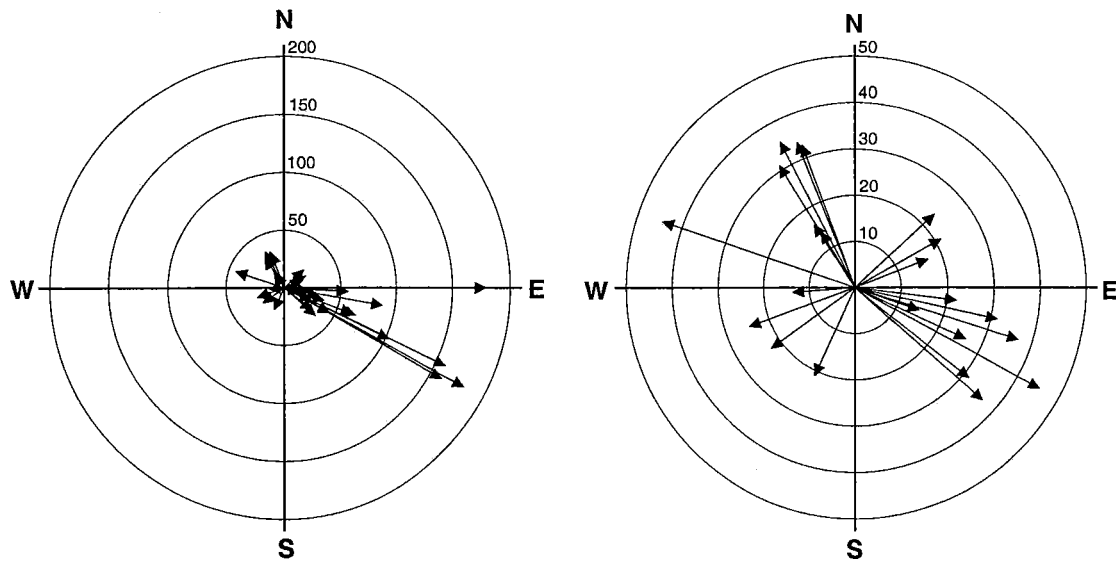


Fig. 6.1.6. Location differences (in km) and azimuthal directions of the NORSTAR GBF solutions with regard to the local solutions. The plot to the left contains all solutions, extending up to 200 km, while the plot to the right contains only events with location differences less than 50 km.